ELSEVIER

Journal of Chromatography A, 721 (1996) 187–201

JOURNAL OF CHROMATOGRAPHY A

Optimum liquid and solid-phase velocity for minimum shock layer thickness in counter-current chromatography

Guoming Zhong[a,b], Georges Guiochon[a,b,*]

[a]*Department of Chemistry, University of Tennessee, Knoxville, TN 37996-1600, USA*

[b]*Division of Chemical and Analytical Sciences, Oak Ridge National Laboratory, Oak Ridge, TN 37831-6120, USA*

First received 25 April 1995; revised manuscript received 12 July 1995; accepted 14 July 1995

Abstract

The shock-layer theory is applied to counter-current liquid chromatography, in the single-component case. This model uses a Langmuir isotherm to account for nonlinear effects, a finite axial dispersion coefficient and a linear driving force (LDF) kinetics to account for the nonideal effects, e.g., the axial dispersion and the mass transfer resistance. The shock-layer velocity and its thickness are explicitly formulated in closed forms. Based on these expressions, the optimum velocities of the solid and liquid phases are derived for minimum shock-layer thickness.

Keywords: Counter-current chromatography; Shock layer thickness; Liquid phase velocity; Solid phase velocity; Thermodynamic parameters

1. Introduction

Continuous separation processes enjoy enormous advantages over classical batch ones for all types of industrial applications. Accordingly, counter-current chromatography and its most practical implementation, simulated moving bed separation (SMB), are topics of great current attention in the separation sciences [1–4].

The development of new separation methods using SMB requires an accurate modeling of this process. It has been reported that the optimum flow-rates of the feed and the solvent observed in SMB are very sharp and cannot be found simply through a series of trials and errors, except in the simpler cases, when the selectivity, α, is very large compared to 1 [2,5]. Often, the empirical search of these optima would not even converge [5]. By contrast, an advanced knowledge of approximate values of the optimum conditions would allow a rapid fine-tuning of the parameters of the separation. Even in the cases in which the empirical approach would eventually converge, considerable savings in time and wasted chemicals are achieved through the use of initial values calculated from a suitable model. This justifies theoretical investigations aiming at the improvement of our understanding of counter-current chromatography as well as of the SMB process. In a previous study [4], we have discussed the solution of the ideal model in counter-current chromatography in the case of a single com-

* Corresponding author. Address for correspondence: Department of Chemistry, University of Tennessee, Knoxville, TN 37996-1600, USA.

0021-9673/96/$15.00
SSDI 0021-9673(95)00777-6

ponent. The advantage of the ideal model [3] is that it focusses attention on the influence of the thermodynamics of phase equilibrium on the behavior of the band and the general shape of its profile. One of the significant results of our work [4] is the existence of a range of experimental conditions under which the column can be flooded by the feed.

Actual columns have a finite efficiency, however. The concentration shocks predicted by the ideal model never take place. They are eroded by the dispersive effects of the axial dispersion in the liquid phase and of the resistance to mass transfer across the column. Under conditions of strong nonlinear behavior, these shocks are replaced by shock layers [6]. The purpose of the present study is the extension of the shock-layer theory of Rhee et al. [6] and Rhee and Amundson [7,8] to the case of counter-current chromatography. The advantages of this approach are its great simplicity, the fact that, in other modes of chromatography [3,9–11], it gives a closed-form equation for the shock-layer thickness, and that values of the optimum velocity for minimum shock-layer thickness derived from these equations are in good agreement with experimental results [9]. Note, however, that this theory is valid only when the column efficiency is large enough for the product $St \cdot Pe$ to be very large [3,7]. This condition may not be as easily verified in SMB as it is in other modes or implementations of chromatography because experience shows that short columns packed with coarse particles and having a rather low efficiency are sufficient to achieve most separations. On the other hand, the migration distance of a front in SMB can be extremely long. Therefore, the extension of the results obtained for counter-current chromatography to the SMB case may not be straightforward. Even if it were so, however, the results would provide an improved understanding of the nature of the phenomena involved in this new process.

The goal of this paper is to provide an analysis of the shock-layer profile in counter-current chromatography and to determine the experimental conditions allowing the formation of the shock-layer of minimum thickness. This will provide useful guidelines for the improvement of separation performance and, eventually, for the optimization of the experimental conditions in separation systems based on the principle of counter-current chromatography, especially in the case of SMB.

2. Theory

The shock-layer theory requires some minor adjustments for its application to counter-current chromatography. When this is done, it is easy to derive the equation giving the shock-layer thickness as a function of the experimental conditions and to determine the value of these parameters for which it is minimal.

2.1. The model of counter-current liquid chromatography

Mass-balance equation

Because of the movement of the solid phase, an additional convective term is required in this equation [4]. It becomes

$$\frac{\partial C}{\partial t} + u\frac{\partial C}{\partial z} - Fv\frac{\partial q}{\partial z} - D_L\frac{\partial^2 C}{\partial z^2} + F\frac{\partial q}{\partial t} = 0 \qquad (1)$$

where C and q are the concentrations in the liquid- and solid phase, respectively, at time t and position z. D_L is the axial dispersion coefficient, u and v are the velocities of the liquid- and solid phase, respectively, $F = (1 - \epsilon)/\epsilon$ is the phase ratio, and ϵ is the total column porosity.

Mass transfer kinetics

The overall mass balance in the particle is represented by the solid-film linear driving force (LDF) model [3] for the solid phase:

$$\frac{\partial q}{\partial t} - v\frac{\partial q}{\partial z} = k(q^* - q) \qquad (2)$$

where k is the lumped mass transfer rate coefficient in the particle. When $k = \infty$, the two phases are constantly in equilibrium.

Adsorption isotherm

We use in this study the Langmuir adsorption isotherm model

$$q^* = f(C) = \frac{aC}{1 + bC} \tag{3}$$

where q^* is the solid-phase concentration in equilibrium with the liquid-phase concentration C. The parameters a and b are numerical coefficients.

Equations of the model

Eqs. 1 and 2 can be rewritten in dimensionless form as

$$\frac{\partial C}{\partial \tau} + \frac{\partial C}{\partial x} - \beta F \frac{\partial q}{\partial x} - \frac{1}{Pe}\frac{\partial^2 C}{\partial x^2} + F\frac{\partial q}{\partial \tau} = 0 \tag{4}$$

$$\frac{\partial q}{\partial \tau} - \beta \frac{\partial q}{\partial x} = St(f(C) - q) \tag{5}$$

with the dimensionless parameters

$$\tau = ut/L \tag{6a}$$

$$x = z/L \tag{6b}$$

$$\beta = v/u \tag{6c}$$

$$Pe = \frac{uL}{D_L} \tag{6d}$$

$$St = \frac{kL}{u} \tag{6e}$$

where L is the column length, and Pe and St are the Peclet and Stanton number, respectively. Because, from the hydrodynamic point of view, the relevant velocity in counter-current chromatography is the velocity of the liquid relative to the solid particles, it might be more appropriate to use $u + v = (1 + \beta)u$ in the definition of the Peclet and Stanton numbers. However, this does not cause any serious change since the coefficient $1 + \beta$ is constant during any separation run considered. For this reason, we have decided to stick with the symbol definitions which are conventional in the field [1,2].

Initial and boundary conditions

The shock-layer profile is obtained for the classical initial and boundary conditions of the breakthrough profile. The column is initially filled with a solution of concentration C_0 in equilibrium with the solid phase. At the time origin, this solution is abruptly replaced by another one having concentration C_1. So, the conditions are

$$C(\tau = 0, x) = C_0 \tag{7a}$$

$$C(\tau, x = 0) = C_1 \tag{7b}$$

Equilibrium is considered between the two phases, so the corresponding conditions for the solid phase are

$$q(\tau = 0, x) = f(C_0), \tag{7c}$$

$$q(\tau, x = 0) = f(C_1) \tag{7d}$$

Because in counter-current chromatography the front may move either in the direction of the liquid phase or in that of the solid phase, we must consider a column extending from $z = -L$ to $z = +L$, with the feed being injected at the center of the column ($z = 0$).

Shock-layer velocity

The shock-layer profile is an asymptotic solution [3,6]. We assume that the column is long enough to permit the development of a quasi-steady-state profile, the shock layer, which propagates without change, i.e., by translation at a constant velocity. In practice, the breakthrough curves obtained with low-molecular-mass chemicals which have reasonably fast mass transfer kinetics on conventional high-performance liquid chromatography (HPLC) columns satisfy these requirements [9]. With proteins, however, shock layers may be observed less often. There is little information available on this issue at this time.

To obtain the asymptotic solution of the system of equations Eqs. 4–6 with the boundary conditions in Eq. 7, we search for a moving coordinate system ξ:

$$\xi = x - \lambda\tau \tag{8}$$

where λ is constant. If this is possible, then the solution of Eqs. 4–7 can be expressed in the form

$$C(x, \tau) = C(\xi) \tag{9a}$$

$$q(x,\tau) = q(\xi) \tag{9b}$$

The solution must also satisfy the following boundary conditions:

$$C(\xi = -\infty) = C^{\mathrm{I}}, \quad \frac{\mathrm{d}C}{\mathrm{d}\xi}(\xi = -\infty) = \frac{\mathrm{d}q}{\mathrm{d}\xi}(\xi = -\infty) = 0 \tag{10a}$$

$$C(\xi = \infty) = C^{\mathrm{r}}, \quad \frac{\mathrm{d}C}{\mathrm{d}\xi}(\xi = \infty) = \frac{\mathrm{d}q}{\mathrm{d}\xi}(\xi = \infty) = 0 \tag{10b}$$

After some mathematical rearrangements [3,6], it can be shown that the steady-state breakthrough profile is a solution of the following third-order differential equation

$$\frac{\lambda + \beta}{Pe \cdot St}\frac{d^3C}{d\xi^3} - \left[\frac{1}{Pe} + \frac{(\lambda+\beta)(1-\lambda)}{St}\right]\frac{d^2C}{d\xi^2} + (1-\lambda)\frac{dC}{d\xi} - F(\beta+\lambda)\frac{df}{d\xi} = 0 \tag{11}$$

If the product $Pe \cdot St$ is much larger than unity, it is possible to neglect the first term in Eq. 11. This is a coupling term between the effects of axial dispersion and the mass transfer kinetics. When this simplification is legitimate, direct integration of Eq. 11 from $\xi = -\infty$ to ξ, using the first boundary condition (Eq. 10a), is possible. This gives the following first-order differential equation:

$$\left[\frac{1}{Pe} + \frac{(\lambda+\beta)(1-\lambda)}{St}\right]\frac{dC}{d\xi} = (1-\lambda)(C - C^{\mathrm{I}}) - F(\beta+\lambda)(f - f^{\mathrm{I}}) \equiv G(C, C^{\mathrm{I}}, C^{\mathrm{r}}) \tag{12}$$

By applying the second boundary condition (Eq. 10b), we obtain the reduced shock-layer velocity in counter-current chromatography as

$$\lambda = \frac{1 - \beta F\dfrac{f^{\mathrm{I}} - f^{\mathrm{r}}}{C^{\mathrm{I}} - C^{\mathrm{r}}}}{1 + F\dfrac{f^{\mathrm{I}} - f^{\mathrm{r}}}{C^{\mathrm{I}} - C^{\mathrm{r}}}} = \frac{1 - \beta K}{1 + K} \tag{13}$$

Thus, the actual migration velocity of the shock layer is given by

$$u_z = \lambda u \tag{14}$$

This velocity is also the migration velocity along the column of all the intermediate concentrations of the profile and especially of concentrations C^{r} and C^{I}.

Note that the reduced shock-layer velocity in a fixed bed [3,6–8] is

$$\lambda = \frac{1}{1 + F\dfrac{f^{\mathrm{I}} - f^{\mathrm{r}}}{C^{\mathrm{I}} - C^{\mathrm{r}}}} = \frac{1}{1+K} \tag{15}$$

The only difference between these equations is the factor $(1 - \beta K)$ in Eq. 13 for counter-current chromatography. This factor may be positive, negative, or zero. Thus, in counter-current chromatography, the shock layer and the sample wave may move forward in the direction of the liquid phase or backward in the direction of the solid phase or it may stay stagnant. Based on this principle, the continuous separation of a binary mixture can be done by choosing the value of β such that one component moves forward while the other one moves backward. When the counter-current solid velocity is 0, then $\beta = 0$ and the bed becomes a fixed bed. In this case, the factor $(1 - \beta K) = 1$ and Eq. 13 reduces to Eq. 15.

2.2. The shock-layer thickness

From Eq. 12 we can see that both the axial dispersion (proportional to $1/Pe$) and the mass transfer resistance (proportional to $1/St$) contribute to the shock-layer thickness, which is defined as a function of ξ. The contributions of these two phenomena, axial dispersion and mass transfer resistance, to the first-order term of Eq. 12 are additive, assuming that the product of the Peclet and Stanton numbers is large enough to neglect the second-order term, as it is often in practice. Within the range of validity of this assumption, we can calculate the shock-layer thickness, $\Delta\xi(C)$.

Since we are interested in the part of the concentration wave in which the main part of the concentration change takes place, we define boundaries $C^{\mathrm{r}*}$ and $C^{\mathrm{I}*}$ such that $C^{\mathrm{r}*} = \theta C_0$ and $C^{\mathrm{I}*} = (1-\theta)C_0$, where $\theta < 0.5$ is a numerical

parameter. Usually, a value $\theta = 0.05$ is used. Then, the shock-layer thickness is given by

$$\Delta\xi(C) = \left[\frac{1}{Pe} + \frac{(\lambda+\beta)(1-\lambda)}{St}\right] \times \int_{C^{r*}}^{C^{l*}} G^{-1}(C,C^{l},C^{r})\,dC \quad (16)$$

This equation is formally the same as the one obtained for a fixed bed, except that the function $G(C,C^{l},C^{r})$ is different due to the existence of the factor accounting for the velocity of the solid phase in counter-current chromatography.

The function $G(C,C^{l},C^{r})$ can be integrated in the case of a Langmuir isotherm. The analytical solution is

$$\Delta\xi = (1+\beta)^{-1}\left[\frac{1}{Pe} + \frac{(\lambda+\beta)(1-\lambda)}{St}\right] \times \left(1 + \frac{1}{k_0' R^{l} R^{r}}\right)\frac{R^{r}+R^{l}}{R^{r}-R^{l}} \ln\left(\frac{1-\theta}{\theta}\right) \quad (17)$$

where $R^{l} = 1/(1+bC^{l})$ and $R^{r} = 1/(1+bC^{r})$.

In the case of a fixed bed we have $\beta = 0$ and Eq. 17 reduces to

$$\Delta\xi = \left[\frac{1}{Pe} + \frac{\lambda(1-\lambda)}{St}\right] \times \left(1 + \frac{1}{k_0' R^{l} R^{r}}\right)\frac{R^{r}+R^{l}}{R^{r}-R^{l}} \ln\left(\frac{1-\theta}{\theta}\right) \quad (18)$$

This is the equation previously derived for the shock-layer thickness in fixed-bed chromatography, with a Langmuir isotherm [3,6–10]. The only formal difference between Eqs. 17 and 18 arises from the presence of β in the former equation. However, the reduced velocity of the shock layer, λ, in Eq. 17 is also a function of the velocity ratio β.

The actual thickness (SLT) in length units of the shock layer migrating along the column can be derived from Eq. 17. It is

$$\Delta x = \left[\frac{1+K}{K \cdot Pe(1+\beta)} + \frac{1+\beta}{St(1+K)}\right] \times \frac{2 + b(C^{l}+C^{r})}{b(C^{l}-C^{r})} \ln\left(\frac{1-\theta}{\theta}\right) \quad (19)$$

2.3. Optimum velocity for minimum shock-layer thickness

Since the shock-layer thickness is given by a closed-form equation, it is straightforward to derive directly from this expression the optimum velocities of the liquid- and solid phase for minimum shock-layer thickness.

Optimum liquid-phase velocity for a given β

The shock-layer thickness (Eq. 19) is a function of the liquid-phase velocity through the Peclet and the Stanton numbers (Eqs. 6d and 6e). Furthermore, the apparent axial dispersion coefficient, D_L, in the Peclet number is also a function of this velocity. Replace D_L by the Van Deemter relationship, $2D_L = Au + 2\gamma D_m$. Differentiating Eq. 19 with respect to u after these rearrangements is done, and setting the differential equal to zero gives the optimum velocity of the liquid phase:

$$u_{opt} = \frac{1+K}{1+\beta}\sqrt{\frac{\gamma D_m k}{K}} \quad (20)$$

In this derivation, β is kept constant, which means that the ratio of the liquid- and solid-phase velocities remains constant. Introducing u_{opt} into Eq. 19 gives the minimum value of the shock-layer thickness:

$$\Delta x|_{min}^{u} = \frac{1}{L}\left[\frac{A(1+K)}{2K(1+\beta)} + 2\sqrt{\frac{D_m \gamma}{kK}}\right] \times \frac{2 + b(C^{l}+C^{r})}{b(C^{l}-C^{r})} \ln\left(\frac{1-\theta}{\theta}\right) \quad (21)$$

Note that the minimum shock-layer thickness obtained decreases monotonically with increasing value selected for β.

Optimum solid-phase velocity for a given u

If we consider the liquid flow velocity, u, as constant, St and Pe in Eq. 19 are also constant. Changing the solid-phase velocity is the same as changing the velocity ratio β. The optimum value of β for minimum shock-layer thickness is obtained by setting equal to 0 the differential of the SLT with respect to β:

$$\beta_{opt} = (1+K)\sqrt{\frac{St}{K \cdot Pe}} - 1 = \frac{1+K}{u}\sqrt{\frac{kD_L}{K}} - 1 \tag{22}$$

The corresponding minimum shock-layer thickness is

$$\Delta x|^{\beta}_{min} = \frac{2}{\sqrt{Pe \cdot St \cdot K}} \frac{2 + b(C^l + C^r)}{b(C^l - C^r)} \ln\left(\frac{1-\theta}{\theta}\right)$$

$$= \frac{2}{L}\sqrt{\frac{D_L}{kK}} \frac{2 + b(C^l + C^r)}{b(C^l - C^r)} \ln\left(\frac{1-\theta}{\theta}\right) \tag{23}$$

The minimum shock-layer thickness depends on the constant value selected for the velocity u only through the apparent axial dispersion coefficient. It decreases monotonically with decreasing value of u.

The shock layer (or the sample) may move forward or backward in the column, depending on the sign of λ (Eq. 13), i.e., on that of $1 - \beta K$. Thus, it is interesting to examine in which direction the shock layer of minimum thickness moves. Introducing β_{opt} into Eq. 13 gives

$$\lambda_{opt} = 1 - \sqrt{\frac{K \cdot St}{Pe}} \tag{24}$$

Eq. 24 shows that the reduced velocity, λ_{opt}, of the shock layer of minimum thickness, corresponding to the optimum value, β_{opt}, of β is positive and the shock layer moves forward if $K < Pe/St$. Conversely, the optimum solid-phase velocity or β_{opt} cannot be obtained for a forward moving shock layer with minimum thickness if $K > Pe/St$. In this latter case, we can only obtain a shock layer of minimum thickness for a backward moving shock layer. Thus, if the values of K, Pe, and St (hence u) are fixed, the optimum value, β_{opt}, can be achieved only in one direction of shock-layer propagation.

Simultaneous optimization of u and β

In practice, we are not interested only in changing u at constant β and β at constant u, but also in the absolute optimum obtained by adjusting simultaneously u and either v or β, in order to achieve the absolute minimum shock-layer thickness possible. Examination of Eqs. 21 and 23 shows that this condition is achieved for

$$u = 0$$

$$\beta = \infty$$

$$with \quad u(1+\beta) = (1+K)\sqrt{\frac{\gamma D_m k}{K}} \tag{25}$$

and the corresponding minimum shock-layer thickness is

$$\Delta x_{opt} = \frac{2}{L}\sqrt{\frac{D_m \gamma}{kK}} \frac{2 + b(C^l + C^r)}{b(C^l - C^r)} \ln\left(\frac{1-\theta}{\theta}\right) \tag{26}$$

This solution is singular and impractical. A zero liquid-phase velocity is meaningless in practice, as it does not permit the production of an extract. An infinite solid-phase velocity is also meaningless. Despite this, this result affords a useful guideline. The value of the constant velocity ratio selected for the optimization of the liquid-phase velocity should be as large as reasonably possible. Conversely, the value of the constant liquid-phase velocity chosen for the optimization of the solid-phase velocity should be as low as possible.

Nature of the steady state

In a column of fixed length, the shock will move forward if the optimum conditions given by Eq. 20 or 22 correspond to a positive optimum value of λ. Then, the shock will move along the column until it reaches its exit. Similarly, if λ_{opt} is negative, the shock will move backward, toward the liquid-phase inlet, and exit this way. When the shock layer has left the column, the steady state corresponds to the elution of a plateau of constant concentration height. Since the shock layer has disappeared, its thickness is no longer meaningful and relevant. This is the case in true moving-bed separation systems, in which case the shock layer is useful only in considering the transition to the steady state.

In simulated moving bed, however, the actual column is divided into a series of individual columns which are switched at a constant frequency. Every time the switching valves are actuated, a new, clean column is placed at the column exit, so for all practical purposes, the column length appears to be infinite and the shock layer never reaches its end. During a

switching period, the whole set of concentration profiles, hence the shock layer, moves a distance equal to one individual column length. Therefore, the shock-layer concept appears to be most germane to an understanding of the behavior of SMB. The shock-layer thickness determines the length of column occupied by the front and, thus, the bed characteristics and the operating conditions required to avoid that the shock layer extends too far beyond the desorbent point and extract points. The conditions of minimum shock-layer thickness will provide a good starting point for the optimization of SMB operation.

2.4. Illustrations and discussion

The system of equations Eqs. 5–7 was solved numerically using a finite-difference method [3]. Calculations were made to illustrate the theoretical results obtained above. The concentration profiles along the column are plotted and discussed. The parameters used in the calculations are: phase ratio, $F = 0.25$; concentration step change, $C_0 = 0$, $C_1 = 25$ mg/ml; Langmuir isotherm, $a = 2$ and $b = 0.02$ ml/mg; the ratio of the intermediate boundary concentration over the boundary concentration, $\theta = 0.05$.

Forward moving concentration profiles

Forward propagation of the shock layer requires that the shock velocity be positive. As shown by Eq. 13, this means that $\beta < 1/K$. Thus, β should be small, the solid phase must move relatively slowly with respect to the liquid phase. We first examine the effect of the velocity ratio β, then discuss the influence of the kinetic parameters, apparent axial dispersion coefficient and mass transfer kinetics rate constant, and the values of the optimum velocities of both phases.

It is useful to point out at this stage that when the composition of the feed stream injected in the center of a chromatographic column is changed, two concentration profiles are formed, one in the front (direction of the liquid phase), the other in the back (direction of the solid phase). Depending on the specifics of the case, one front is stationary, the other moves; one front is a shock layer, the other is diffuse. In the case of a Langmuir isotherm and $\beta < 1/K$, a shock layer propagates in the same direction as the mobile phase while a diffuse, stationary, steady-state front is formed in the region $z < 0$, close to the origin, where the incoming mobile phase strips the compound from the stream of solid phase. The profile of this front could be obtained by writing the balance between the backward flux brought by the solid phase and the forward flux caused by the liquid stream [12]. This study is not part of our goal. Fig. 1a illustrates this situation and shows the two concentration profiles at three successive times. The rear, stationary, diffuse front is at the origin. The shock layer migrates in the positive direction. The shock layer is thicker than the diffuse front because of the self-sharpening effect arising in the formation of steady zones [12]. Conversely, when $\beta > 1/K$, the diffuse front moves backward, in the direction of the solid phase and the shock layer is stationary and positioned at the origin. This is because, with a Langmuir isotherm, the shock layer originates from the front shock of the injection band, which is self-sharpening, while the diffuse boundary originates from the rear shock [4].

If the equilibrium isotherm follows an anti-Langmuir behavior, the opposite results are found. When $\beta < 1/K$, a diffuse boundary moves in the forward direction, with the liquid phase, while a fixed shock layer is located at the origin. By contrast, if $\beta > 1/K$, a shock layer moves in the backward direction, with the solid phase, while a stable diffuse boundary remains located at the origin. Fig. 1b illustrates this situation. The rear part of the rear profile has not yet completely stabilized because this is an asymptotic solution and a certain time is needed to approach it closely enough.

Influence of the ratio of the liquid and solid velocities, β

Fig. 2a shows the concentration profiles along the column at time $\tau = t/t_0 = 1$ for different values of β: 0.0 (fixed bed), 0.5, 1.0, and 1.5. The axial dispersion is characterized by the Peclet number $Pe = 200$ and the mass transfer resistance by the Stanton number $St = 1000$. In this

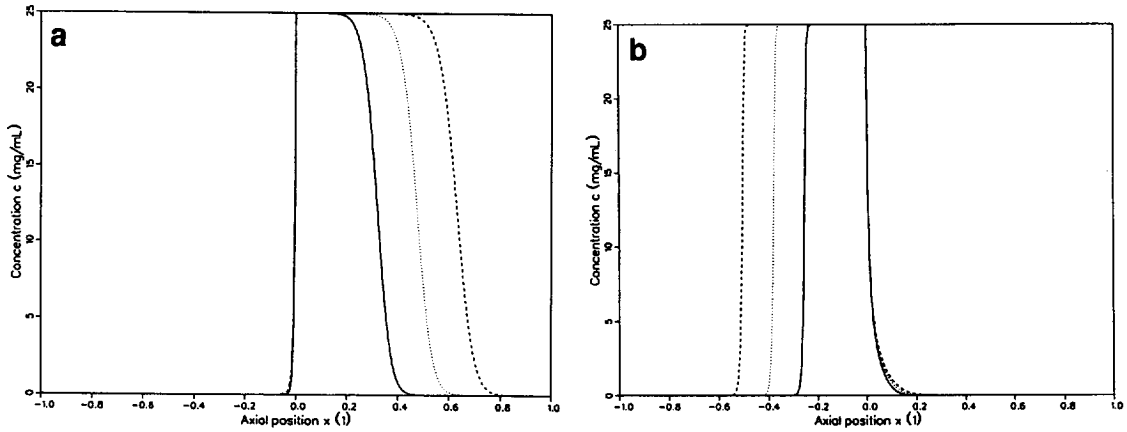

Fig. 1. Illustration of the two boundaries formed during the injection of a concentration step in counter-current chromatography. (a) Langmuir isotherm, $\beta = 0.5$, $Pe = 200$, $St = 1000$. Profiles calculated for $\tau = 0.5$ (solid line), 0.75 (dotted line), and 1.0 (dashed line). (b) Anti-Langmuir isotherm, $\beta = 2.0$, $Pe = 200$, $St = \infty$. Profiles calculated for $\tau = 0.5$ (solid line), 0.75 (dotted line), and 1.0 (dashed line).

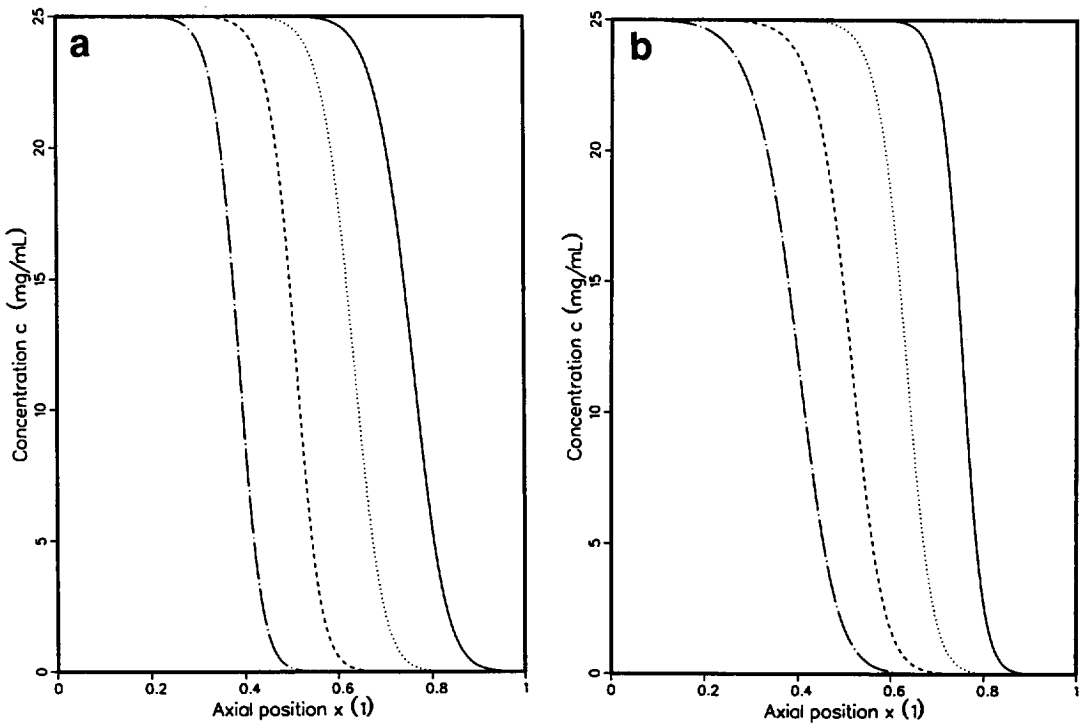

Fig. 2. Forward moving profiles. Influence of the ratio of the solid- and liquid-phase velocities. Axial profiles registered at time $\tau = 1.0$. Solid line, $\beta = 0.0$ (fixed bed); dotted line, $\beta = 0.5$; dashed line, $\beta = 1.0$; chain-dotted line, $\beta = 1.5$. (a) $Pe = 200$, $St = 1000$; (b) $Pe = 1000$, $St = 100$.

case, the mass transfer is faster than the axial dispersion, and the latter is the limiting factor. In Fig. 2a, the larger β, the faster the solid phase migrates in the direction opposite to that of the shock-layer propagation, and the slower the concentration profile migration (see Eq. 13). Also, the larger β, the smaller the shock-layer thickness, Δx. This is in agreement with Eq. 19, where *St* being large and *Pe* small, the first term, inversely proportional to $(1+\beta)$, is dominant. The values of the shock-layer thickness[1] calculated from Eq. 19 are respectively 0.29, 0.21, 0.17, and 0.14 for $\beta = 0.0$, 0.5, 1.0, and 1.5, in good agreement with those derived from the results of the numerical calculations, which are 0.22, 0.18, 0.16, and 0.14, respectively.

Conversely, if the effect of mass transfer is dominant compared to that of axial dispersion, the opposite influence of β on the shock-layer thickness is found. In Fig. 2b, $Pe = 1000$ and $St = 100$. In this case, the larger β, the larger the shock-layer thickness, Δx, in agreement with Eq. 19, in which the *St* term is proportional to $1+\beta$. The values obtained from numerical calculations are respectively 0.14, 0.18, 0.22, and 0.26 for $\beta = 0.0$, 0.5, 1.0, and 1.5, while the analytical solution (Eq. 19) gives 0.16, 0.20, 0.25, and 0.30, respectively.

Influence of axial dispersion and mass transfer resistance

As in the fixed-bed case, axial dispersion and mass transfer resistance have no influence on the propagation velocity of the shock layer, which remains the same as the velocity of the shock in the ideal case [3,6–8]. They are responsible for the transformation of the concentration shock into a shock layer and they control the width of the concentration profiles. Fig. 3a shows the effect of changing the apparent axial dispersion coefficient. The Peclet number *Pe* for the four curves is respectively 100, 200, 300 and 500. The corresponding shock-layer thickness obtained from the analytical solution of Eq. 19 is 0.31, 0.17, 0.12, and 0.052, respectively, and 0.25, 0.16, 0.12, and 0.056 when derived from the numerical calculations. The larger the Peclet number, i.e., the smaller the dispersion coefficient, the sharper the concentration profile. Fig. 3b shows the similar effect of the mass transfer kinetics, through changes in the value of *St*, the Stanton number. The larger *St*, the steeper the profiles. The value of *St* is respectively 150, 250, 400 and 1000 for the four profiles in Fig. 3b. The shock-layer thickness calculated from the solution of Eq. 19 is 0.16, 0.12, 0.087, and 0.056, respectively, while values of 0.17, 0.12, 0.085, and 0.052 are obtained from the numerical calculations of these profiles.

The similarity in the behavior of the shock-layer profile and thickness when axial dispersion and mass transfer kinetic resistance are changed is in agreement with Eq. 19. It originates in the symmetry between the influence of these two phenomena found in Eq. 11. Neglecting the coupling term in this equation causes their respective contributions to the shock-layer thickness to be simply additive.

Optimum velocities

The most important result derived from the theoretical study made in this work is the calculation of the values of the optimum liquid- and solid-phase velocities for minimum shock-layer thickness, based on Eq. 19. This result is illustrated in Fig. 4, in which the concentration profiles obtained at different values of the liquid-phase velocity, for a constant phase velocity ratio β are plotted. The values selected for β are 0.5 in Fig. 4a and 1.5 in Fig. 4b. Other parameters used in Eqs. 20 and 21 to calculate these profiles are the column length, $L = 10$ cm, the mass transfer kinetic coefficient, $k = 1\ s^{-1}$, the thermodynamic constant, $K = 1/3$, and the constants $A = 0.002$ and $2\gamma D_m = 0.0005\ cm^2/s$ of the Van Deemter's equation.

With these parameters, the optimum liquid velocity for $\beta = 0.5$ is $u = 0.024$ cm/s (solid line in Fig. 4a) and for $\beta = 1.5$ it is $u = 0.015$ cm/s (solid line in Fig. 4b). In order to illustrate the variations of the profiles around the optimum velocity for minimum SLT, two other values of

[1] The numerical values given in the text for SLT are in units of x (Eq. 6b), hence they are dimensionless.

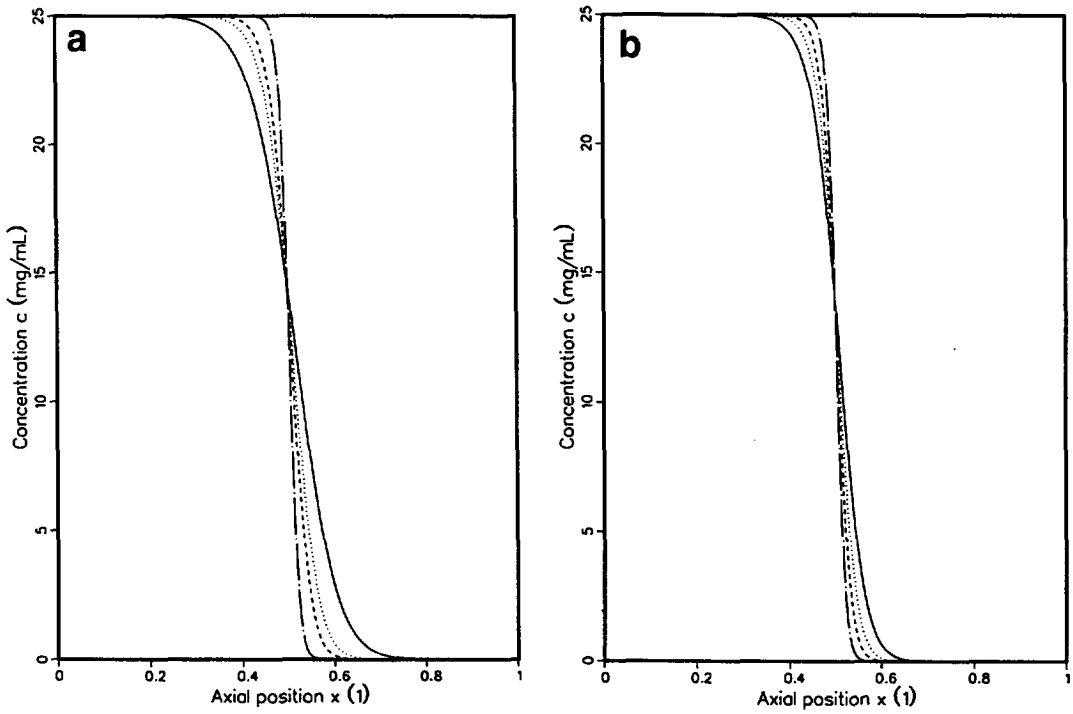

Fig. 3. Forward moving profiles. Influence of axial dispersion and mass transfer resistance. Axial profiles registered at time $\tau = 1.0$, for $\beta = 1.0$. (a) Influence of axial dispersion ($St = 1000$). Solid line, $Pe = 100$; dotted line, $Pe = 200$; dashed line, $Pe = 300$; chain-dotted line, $Pe = 500$. (b) Influence of the mass transfer kinetic resistance ($Pe = 1000$). Solid line, $St = 150$; dotted line, $St = 250$; dashed line, $St = 400$; chain-dotted line, $St = 1000$.

the liquid-phase velocity were chosen and the corresponding profiles are also plotted in each figure. These values are $u = 0.014$ cm/s (dotted line) and 0.034 cm/s (dashed line) in Fig. 4a and $u = 0.0046$ (dotted line) and 0.025 cm/s (dashed line) in Fig. 4b. While it is obvious that the solid lines in the two figures have the sharpest profiles, it is also clear that the optimum is not sharply defined.

Finally, Fig. 4c shows the profile obtained with the optimum solid-phase velocity for the liquid-phase velocity corresponding to $Pe = 200$ and $St = 200$. The optimum solid-phase velocity given by Eq. 22 corresponds to $\beta = 0.63$. No other profile corresponding to a value of β either larger or lower than the optimum is plotted for comparison because such profiles would be too close to the optimum one. This illustrates how weakly defined the optimum is in this case.

Backward moving concentration profiles

When the solid phase moves quickly enough in the direction opposite to that of the liquid-phase flow, i.e., when β is large enough, λ in Eq. 13 is negative. Then, the propagation of the concentration profile takes place in the same direction as the movement of the solid phase, i.e, in the backward direction, instead of the forward direction, that of the liquid phase [4]. The condition to have backward migration of the shock layer is that $\beta > 1/K$. In this case, the study of the propagation of the shock layer requires that the column extends toward negative values of z, to e.g., $z = -L$ (Eq. 7b). The properties of the SLT are similar to those discussed in the previous section. The effects of axial dispersion and the mass transfer resistance on the shock-layer thickness are similar to those found in the case of the forward moving profiles and do not need to be

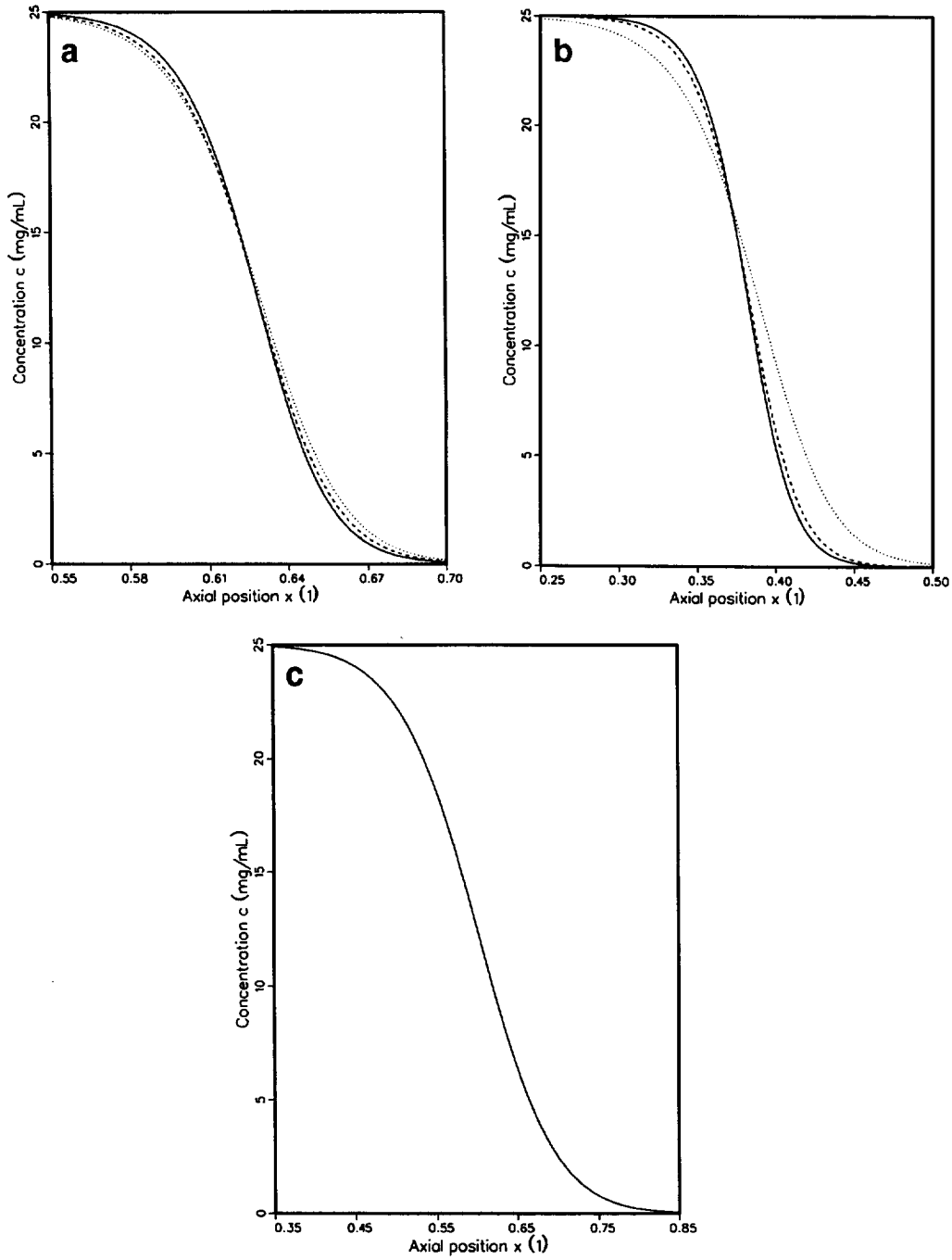

Fig. 4. Forward moving profiles. Profiles at the optimum velocities. Column length $L = 10$ cm, mass transfer coefficient $k = 1\ s^{-1}$, constant $K = 1/3$, constants $A = 0.002$ and $2\gamma D_m = 0.0005\ cm^2/s$. All axial profiles are at time $\tau = 1.0$. (a) $\beta = 0.5$. Solid line, optimum liquid-phase velocity, $u = 0.024$ cm/s; two other velocities for comparison: dotted line, $u = 0.014$ cm/s and dashed line, $u = 0.034$ cm/s. (b) $\beta = 1.5$. Solid line, optimum liquid-phase velocity, $u = 0.015$ cm/s; two other velocities for comparison: dotted line, $u = 0.0046$ cm/s and dashed line, $u = 0.025$ cm/s. (c) Profile obtained for the optimum solid-phase velocity $\beta = 0.63$. The liquid-phase velocity is constant and corresponds to $Pe = 200$ and $St = 100$.

illustrated again here. The same is true for optimum velocities.

In the previous case, the positive step change $C_1 = 25$ mg/ml at the inlet ($x = 0$) of an initially empty column (Eq. 7a) caused the formation of a steady concentration front (or shock layer) moving in the forward direction. Under the same Langmuir isotherm, the same step change causes now a diffuse profile to migrate in the forward direction, as shown in Fig. 5, in which the axial concentration profile is plotted at two different times, $\tau = 0.5$ and 1.0. The other parameters used in these calculations are $Pe = 200$, $St = \infty$, and $\beta = 4.0$. It is obvious that no shock layer with constant pattern will be formed. This is due to the thermodynamic properties of the column with the Langmuir-type isotherm, and is explained in detail in our previous paper [4].

However, a shock layer propagating in the backward direction will be observed in the case of a convex downward isotherm, e.g., an anti-Langmuir isotherm (e.g., with $b = -0.02$ ml/mg). In this case, it is the rear of the rectangular injection of quasi-infinite width which is self-sharpening [4], and it moves in the backward direction, with the solid phase. The front of this injection tends to move forward, with the liquid phase, but it is diffuse because of the negative curvature of the isotherm and it remains stationary, at the origin, as illustrated in Fig. 1b. Figs. 6a and 6b show, at time $\tau = 0.5$, the shock layers obtained for different values of β: 2.0, 2.5, 3.0, and 3.5. Fig. 6a corresponds to $Pe = 200$ and $St = \infty$, Fig. 6b to $Pe = 100$ and $St = 100$ and gives profiles which are much less steep than those in Fig. 6a.

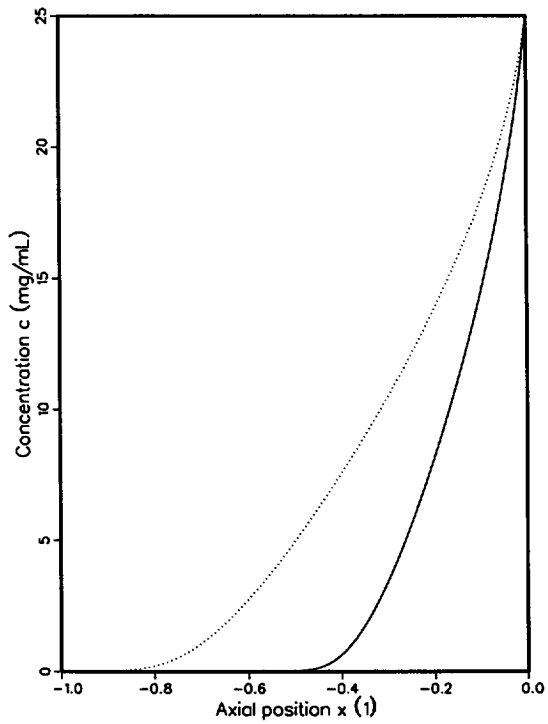

Fig. 5. Case of backward moving profiles. Forward moving diffuse concentration profiles. Concentration step change at the inlet ($x = 0$) of an empty column. A backward moving shock layer is formed. A forward moving constant pattern profile (shock layer) cannot form; the profile is dispersive and broadens with increasing time. Solid line, time $\tau = 0.5$; dotted line, time $\tau = 1.0$. Peclet number $Pe = 200$ and Stanton number $St = \infty$.

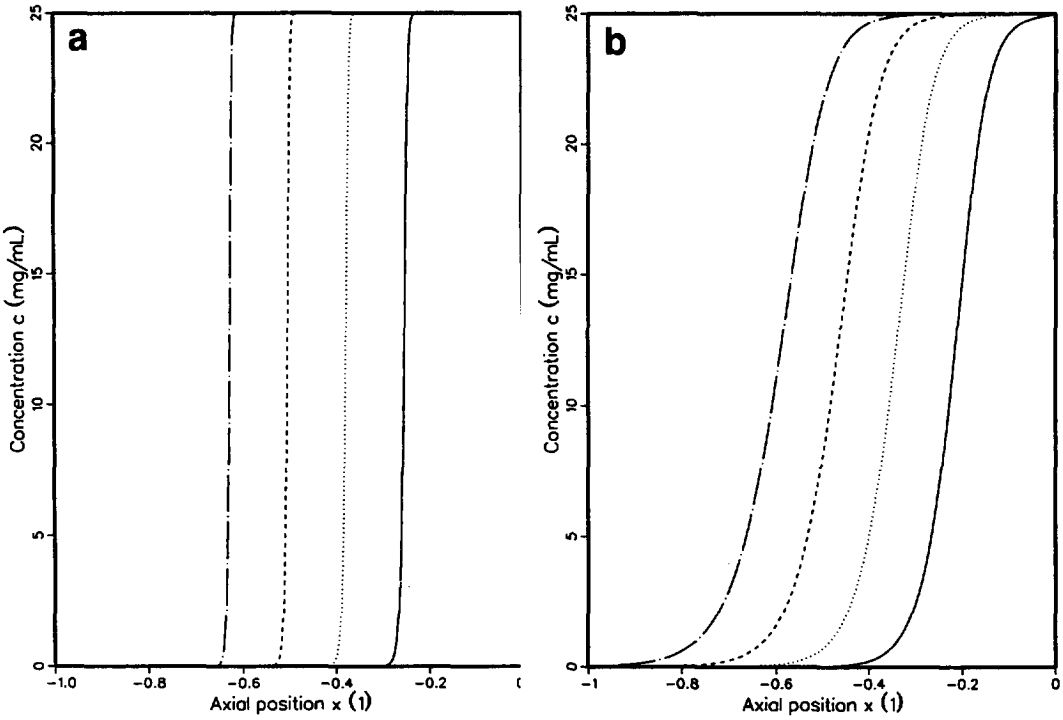

Fig. 6. Case of backward moving profiles. Forward moving shock layer with an anti-Langmuir isotherm. An anti-Langmuir isotherm with $B = -0.02$ is considered. A stable shock layer moves forward. $\tau = 0.5$. Solid line, $\beta = 2.0$; dotted line, $\beta = 2.5$; dashed line, $\beta = 3.0$; chain-dotted line, $\beta = 3.5$. (a) $Pe = 200$, $St = \infty$; (b) $Pe = 100$, $St = 100$.

Similarly, a shock layer can be formed and propagate in the forward direction in the case of a Langmuir isotherm if a negative concentration step is performed, with a column initially saturated at a constant concentration $C_0 = 25$ mg/ml. Than $C^l = 23.75$ and $C^r = 1.25$ mg/ml ($\theta = 0.05$). The reason is that, in this case, low concentrations move faster in the forward direction than high concentrations, so concentrations pile up forward and form a shock layer [4]. Fig. 7 shows the shock layers obtained for $\beta = 4.0$, 4.5, 5.0, and 5.5 at time $\tau = 1.0$, with $Pe = 200$ and $St = \infty$.

The influence of β on the shock-layer thickness is illustrated in Figs. 6a and 7. The SLT decreases with increasing β because of the dominance of the contribution of Pe to the SLT. However, the converse effect is seen in Fig. 6b because, in this case, the contribution of St in Eq. 19 is more important than that of Pe.

3. Conclusion

The results presented in this work open a new approach to the investigation of the behavior of SMB and of the optimization of its operating conditions. The shock layer must remain completely included inside the volume of an individual column when the steady state is reached. Further results on the investigation of this problem will be reported soon [13].

Acknowledgements

This work has been supported in part by Grant CHE-9201663 of the National Science Foundation and by the cooperative agreement between the University of Tennessee and the Oak Ridge National Laboratory. We acknowledge support of

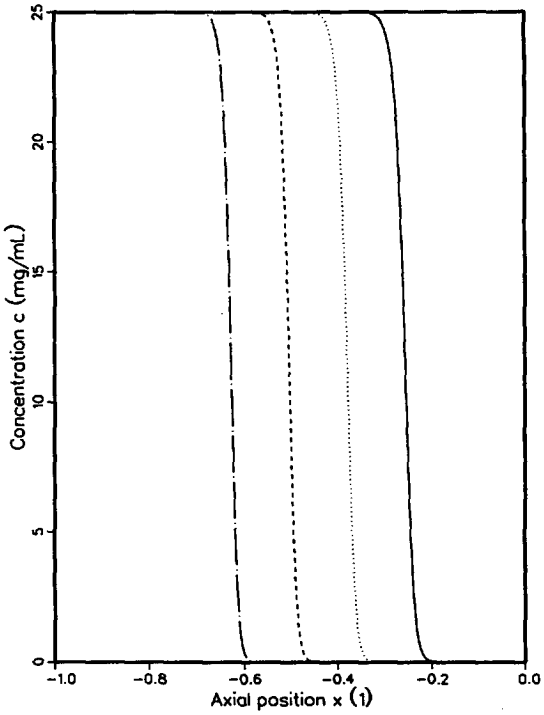

Fig. 7. Case of backward moving profiles. Shock layer observed with a Langmuir isotherm and a purge step (concentration decreasing from 25 to 0 mg/ml). A constant shock layer is formed. $\tau = 1.0$, $Pe = 200$, and $St = \infty$. Values of $\beta =$ 4.0, 4.5, 5.0, and 5.5.

our computational effort by the University of Tennessee Computing Center.

List of symbols

a,b	first and second parameters of the Langmuir isotherm
A	parameter in Van Deemter's equation
C	liquid-phase concentration of the component
C^{l}	left boundary concentration
C^{r}	right boundary concentration
D_L	axial dispersion coefficient
D_m	molecular diffusion in Van Deemter's equation
F	phase ratio
G	function defined by Eq. 12
k	mass transfer coefficient
k'_0	retention factor at infinite dilution ($=Fa$)
K	constant defined by Eq. 13
N	column efficiency
Pe	Peclet number ($=uL/D_L$)
q	solid-phase concentration
R	intermediate parameter [$=1/(1+bC)$]
St	Stanton number ($=kL/u$)
t	time
u	liquid-phase flow velocity
u_z	shock-layer propagation velocity
v	solid-phase flow velocity
x	dimensionless axial position in the column ($=z/L$)
z	axial position in the column

Greek symbols

β	ratio of the solid- and liquid-phase velocities ($=v/u$)
γ	constant in Van Deemter's equation
λ	reduced propagation velocity of shock layer
τ	dimensionless time ($=ut/L$)
θ	coefficient defining the thickness of the shock layer $[=(C^{l}-C^{l*})/(C^{l}-C^{r})=(C^{r*}-C^{r})/(C^{l}-C^{r})]$
ξ	coordinate transform parameter in Eq. 8

References

[1] D.M. Ruthven and C.B. Ching, Chem. Eng. Sci., 44 (1989) 1011.
[2] G. Ganetsos and P.E. Barker, Preparative and Production Scale Chromatography, Marcel Dekker, New York, 1993.
[3] G. Guiochon, S. Golshan Shirazi and A.M. Katti, Fundamentals of Preparative and Nonlinear Chromatography, Academic Press, Boston, MA, 1994.
[4] G.M. Zhong and G. Guiochon, J. Chromatogr. A, 688 (1994) 1.
[5] R.M. Nicoud, Proceedings of the European meeting on Simulated Moving Bed: Basics and Applications, SEPAREX and ENSIC, Nancy, 1993, p. 54.
[6] H.-K. Rhee, Bodin and N.R. Amundson, Chem. Eng. Sci., 26 (1971) 1571.
[7] H.-K. Rhee and N.R. Amundson, Chem. Eng. Sci., 27 (1972) 199.
[8] H.-K. Rhee and N.R. Amundson, Chem. Eng. Sci., 28 (1973) 55.

[9] J. Zhu, Z. Ma and G. Guiochon, Biotechnol. Progr., 9 (1993) 421.
[10] J. Zhu and G. Guiochon, J. Chromatogr., 636 (1993) 189.
[11] J. Zhu and G. Guiochon, AIChE J., 41 (1994) 45.
[12] J.C. Giddings, Unified Separation Science, Wiley, New York, 1991, pp. 112–119.
[13] G.M. Zhong and G. Guiochon, in preparation.